Supporting Information for

Perturbation Approach for Computing Infrared Spectra of Local Molecular Vibrations

Rui-Jie Xue,[1] Adam Grofe,[2] He Yin[1], Zexing Qu,[1] Jiali Gao,[*,1,2] and Hui Li,[*,1]

1. Institute of Theoretical Chemistry, Jilin University, 2519 Jiefang Road, Changchun 130023, People's Republic of China
2. Department of Chemistry and Supercomputing Institute, University of Minnesota, Minneapolis, Minnesota 55455, U.S.A.

E-mail: Prof_huili@jlu.edu.cn and gao@jialigao.org

1. Convergence of the PODVR method

For the $HCl(H_2O)_1$ complex, the transition frequencies of the HCl stretch vibration are listed in Table S1. These frequencies are obtained at the optimized structure of $HCl(H_2O)_1$ complex at CCSD(T)-F12b/cc-pVTZ-F12 level. The non-perturbation transition frequencies are generated directly by solving the one-dimensional Schrödinger equation. Spline interpolation was used to generate the potential over 30 potential grids of HCl stretching coordinate ranging from 0.8 Å to 2.25 Å with equal step of 0.05 Å, and the other degrees of freedom stay constant at the optimized structure of $HCl(H_2O)_1$. All the potential energies are calculated at CCSD(T)-F12b/cc-pVTZ-F12 level.

As shown in table S1, we can find that the non-perturbation energy is convergent at 8 DVR grids. Here, the convergence means that the difference between the non-perturbation energy by PODVR method and the exact value of the transition frequency is less than 1 cm^{-1}. The exact value of the transition frequency is obtained by performing LEVEL program (see: http://scienide2.uwaterloo.ca/~rleroy/level/)

using iteration-variation procedure for solving the Schrödinger equation to make the eigenvalue convergent to 10^{-6} cm^{-1}. The potential energy used in LEVEL program is obtained by least squares fitting energies with polynomial functions. The fit of 30 points, varying from 0.8Å to 2.25 Å, has root-mean-square (RMS) of 0.042 cm^{-1}, requires 11 parameters.

Table S1. The non-perturbation transition frequencies of the HCl stretch vibration are calculated at the optimized structure of $HCl(H_2O)_1$ complex with the increasing number of DVR grids.

DVR grids	Frequency (cm^{-1})
4	2571.06
5	2636.56
6	2647.19
7	2649.68
8	2650.55
9	2650.82
10	2650.92
15	2650.94
20	2650.96
30	2650.91
35	2650.93
40	2650.94
50	2650.94
Exact Result[a]	2650.94

[a] Obtained by using the Level Program

2. Convergence of the quantum vibrational perturbation (QVP) method

Two different perturbation strategies are elaborated with the potential surface calculated at CCSD(T)-F12B/cc-pVTZ-f12 level. In order to obtain the transition frequency of HCl stretch vibration within complex system, the referenced (unperturbative) wave functions of the two perturbation strategies are calculated based on an isolated HCl molecule and a referenced $HClH_2O$ structure respectively. 40 selected structures of the HCl-H_2O complexes which are obtained from the molecular dynamical trajectory between 5ps-6ps with equal time step are tested by the two different perturbation approaches.

The first strategy is that we get the referenced wave functions of the ground and first excited states represented by the DVR grids for an isolated HCl molecule. Then the energy level shift of the υ th state can be expressed as

$$\Delta V_{\upsilon}(R_j) = \int dQ \varphi_{\upsilon}^{*}(Q) \Delta V(R_j, Q) \varphi_{\upsilon}(Q)$$
$$= \sum_{i}^{8} c_{\upsilon i}^{2} \Delta V(R_j, Q_i) \qquad (S1)$$

Here $\Delta V(R_j,Q)$ is the intermolecular energy which is treated as the perturbation term and it's the function of HCl stretch coordinate Q and intermolecular coordinate R_j for the jth instantaneous structure. The weight averaging is implemented using the wave function of the υ th state represented by eight DVR grids.

Here the energy shift of the transition frequency from the first excited state to the ground state is expressed as

$$\Delta\omega_{10} = \frac{\Delta V_1(R_0) - \Delta V_0(R_0)}{\hbar} \qquad (S2)$$

For the second strategy, which is used in the present study, its referenced wave functions for HCl stretching are obtained based on the optimized HCl-water complex. More details have been stated in the main text. The energy shifts of the υ th H-Cl stretch vibrational state of the jth instantaneous structure from the 40 selected structures are

$$\Delta V^{\upsilon}(R_j) = \int dQ \varphi_{\upsilon}^{*}(Q; R_0) \Delta H(R_j, Q) \varphi_{\upsilon}(Q; R_0)$$
$$= \sum_{i}^{8} c_{\upsilon i}^{2} \Delta H(R_j, Q_i) \qquad (S3)$$

where,

$$\Delta H(R_j, Q_i) = H(R_j, Q_i) - H^{0}(R_0, Q_i) \qquad (S4)$$

Here, $H^{0}(R_0,Q_i)$ is the Hamiltonian of the optimized structure with the ith DVR grids of HCl bond and $H(R_j,Q_i)$ is the Hamiltonian of the jth instantaneous structure with the intermolecular coordinates equaling to R_j. The referenced wave function $\varphi_{\upsilon}(Q;R_0)$ of υ th H-Cl stretch vibrational state is obtained at the referenced

intermolecular structure R_0 of HCl-water complex. The calculated transition frequencies of the second perturbation method are given with the label E_{QVP} in the fifth column of Table S2.

The non-perturbation results are obtained from the potential curve which is generated from Splint interpolation on 30 grids of HCl distance scanned from 0.8Å to 2.25Å with the equal step 0.05 Å.

Table S2. Computed vibrational frequencies (cm-1) using the quantum vibrational perturbation (QVP) method and the 1-D vibrational Schrodinger equation (SE).

Structure	E_{SE}	E_{QVP1}	E_{QVP2}	E_{QVP3}	E_{QVP4}
1	2566.45	2570.59	2567.11	2566.86	2566.86
2	2773.97	2781.88	2772.33	2773.51	2773.51
3	2735.80	2739.61	2734.92	2735.34	2735.34
4	2702.77	2704.19	2702.25	2702.37	2702.37
5	2648.65	2648.59	2648.59	2648.59	2648.60
6	2726.42	2729.59	2725.60	2725.94	2725.94
7	2750.80	2756.48	2749.52	2750.30	2750.30
8	2763.04	2769.99	2761.55	2762.56	2762.56
9	2727.82	2730.95	2727.06	2727.38	2727.38
10	2752.38	2758.32	2751.03	2751.87	2751.87
11	2702.70	2704.09	2702.20	2702.32	2702.32
12	2748.59	2753.96	2747.36	2748.08	2748.08
13	2616.01	2616.91	2616.30	2616.28	2616.28
14	2693.88	2694.85	2693.42	2693.50	2693.50
15	2602.15	2603.49	2602.46	2602.43	2602.43
16	2531.72	2539.65	2533.16	2532.51	2532.51
17	2503.59	2515.96	2505.95	2504.69	2504.69
18	2536.07	2543.20	2537.25	2536.70	2536.70
19	2510.26	2521.32	2512.25	2511.19	2511.19
20	2543.66	2550.28	2544.83	2544.33	2544.33
21	2607.54	2608.63	2607.78	2607.74	2607.75
22	2692.31	2693.13	2691.89	2691.96	2691.96
23	2601.02	2602.69	2601.39	2601.32	2601.32

24	2626.41	2626.88	2626.58	2626.58	2626.58
25	2757.76	2764.12	2756.33	2757.26	2757.26
26	2569.08	2573.25	2569.81	2569.55	2569.55
27	2575.52	2579.02	2576.16	2575.96	2575.96
28	2679.86	2680.10	2679.51	2679.54	2679.54
29	2613.08	2613.98	2613.28	2613.26	2613.26
30	2643.22	2643.27	2643.25	2643.25	2643.25
31	2693.88	2694.66	2693.49	2693.55	2693.55
32	2600.65	2602.36	2600.92	2600.84	2600.84
33	2694.03	2694.05	2693.75	2693.76	2693.76
34	2681.15	2681.03	2680.92	2680.92	2680.92
35	2666.98	2666.98	2666.82	2666.82	2666.82
36	2638.83	2638.86	2638.82	2638.82	2638.82
37	2654.45	2654.35	2654.32	2654.32	2654.32
38	2683.89	2684.37	2683.56	2683.60	2683.60
39	2682.68	2683.06	2682.39	2682.41	2682.41
40	2622.01	2622.66	2622.21	2622.20	2622.20
Average	2653.05	2656.03	2652.96	2653.01	2653.01
$Error_{Average}$	0	2.98	-0.09	-0.04	-0.04
RMSD	73.77	73.11	72.92	73.36	73.36

The transition frequencies obtained by solving 1-D vibrational Schrodinger equation are listed in the second column of Table S2. Its average transition frequency is 2653±73.8 cm^{-1}. The corresponding difference between the QVP method and the exact results is about 3.0 cm^{-1}. For comparison, the average frequencies from QVP1, QVP2, QVP3 and QVP4 calculations are 2656.0±73.1 cm^{-1}, 2653.0±72.9 cm^{-1}, 2653.0±73.4 cm^{-1} and 2656.0±73.4 cm^{-1}. Thus, the transition frequencies of the QVP strategy are consistent with that of non-perturbation approach in RMSD. Also, the convergence of perturbation energies is consisted with the enhancement of the perturbation order

According to the above discussion, we find that in the HCl-water strong acid system which has the strong intermolecular interaction and the HCl bond is much easy to be elongated by intermolecular force due to the hydrogen bond. The

intermolecular interaction is too strong to be regarded as the perturbation term in the total Hamiltonian expression, so the second perturbation approach is the much more suitable strategy to deal with the system including strong intermolecular interaction.

3. Ab Initio Molecular Dynamics Simulations Setup

Ab Initio Born-Oppenheimer Molecular Dynamics (BOMD) simulations were performed with the CPMD simulation package (see http://www.cpmd.org/). The BLYP functional corrected by the addition of dispersion interactions[1] was used together with norm-conserving pseudo-potentials for core electrons and the plane wave basis set with cutoff energy of 70 Ry for active valance electrons. The energies, dipole moments and the forces were calculated as the system is propagated in classical molecular dynamics simulations with a time step of 30 au $\approx$ 0.72fs. For all simulations of the systems $(HCl)_m(H_2O)_n$ (m=1,2; n=1,2,3,4), the Nosé-Hoover thermostats[2] were applied in the canonical ensemble (NVT) at 200 K, and coordinates were recorded at step time of 90 au along with the dipole moments). The Poisson equation was solved by using the Martyna-Tuckerman solver[3] for molecules in a cubic box with side-lengths of 15Å. During all simulations the total linear and angular momentum were corrected to zero at every 100 steps.

Analyses of the BOMD trajectories for the $HCl(H_2O)_n$, n = 1 – 4, show that structural variations are consistent with the aggregation-induced chemical reaction mechanism[4,5] on the basis of H_3O^+ formation. Figure S1 shows that the distance H and Cl associated with HCl (red curves) fluctuates at values of 1.3-1.4 Å for n up to 3 in $HCl(H_2O)_n$, but for n = 4, the proton from HCl is equilibrated at a location about equally shared by the chloride ion and a water oxygen atom. This trend is more dramatically reflected in the histograms of the distance between the HCl proton and the nearest oxygen atom of water (blue dashed curves). As n increases from 1 to 4, the distance H_{Cl}-O_w decreases noticeably, eventually reaching a length overlapping with the H_{Cl}-Cl distance (Figure S1d). The results of the Figure S1 indicates that the adjacent O approaches the H atom of the HCl molecule step by step with increasing cluster size of $HCl(H_2O)_n$ until HCl dissociation occurs when a total four water

molecules are added. Figure 1S also indicate that for n = 1, 2 and 3, the HCl molecule remains associated, but dissociation occurs rapidly within 1 ps of simulation time and settles at an equilibrium state after 4 ps. Representative structures in these clusters are shown for each cluster in the corresponding figure in Figure S1. The results mirror that found in previous studies.[6-10]

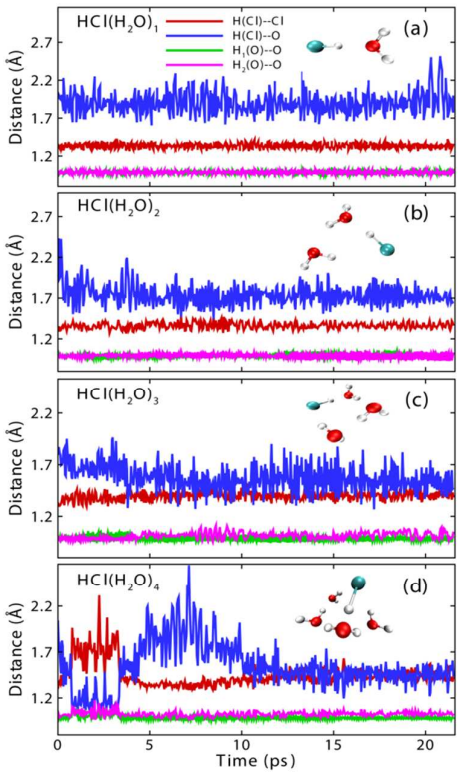

Figure S1. Histogram displaying inter-atomic distances between the acidic proton and Cl atom (red line), the acidic proton and the O atom of the adjacent H_2O (blue line), two H atoms of the adjacent H_2O and the O atom of the adjacent H_2O (green line and pink line)

4. Calculation of 2-Dimensional Infrared (2D-IR) Spectra

The 2D pump-probe spectroscopy is the third-order response function after phase matching. The time t_1 represents the time between the first two pulses, while the time t_2 represents the time between the second two pulses. The results of the signal are

detected at time t_3 after the third pulse, which are converted to the frequency domain using 2D Fourier transforms of time t_1 and t_3[11-13]

$$S_{\mathrm{re}}^{(3)}(\omega_1, t_2, \omega_3) = \int_0^\infty \int_0^\infty R_{re} \cdot \exp[i(\omega_3 t_3 - \omega_1 t_1)]\, dt_3 dt_1 \tag{S5}$$

$$S_{\mathrm{non}}^{(3)}(\omega_1, t_2, \omega_3) = \int_0^\infty \int_0^\infty R_{non} \cdot \exp[i(\omega_3 t_3 + \omega_1 t_1)]\, dt_3 dt_1 \tag{S6}$$

The 2D pump-probe spectrum is obtained as the sum of the imaginary part of both rephrasing signal and non-rephasing signal.[11-13] The response functions of rephrasing R_{re} and non-rephasing R_{non} are determined by instantaneous transition frequencies of 0-1 and 1-2 transition states. Thus, obtaining the precise instantaneous transition frequencies is a crucial step before achieving accurate one or two-dimension IR spectra.

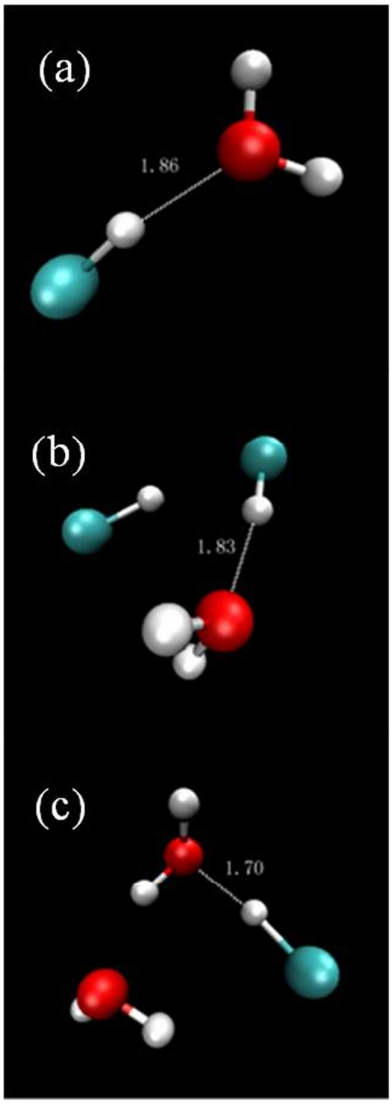

Figure S2. the geometry structures of $HCl(H_2O)$, $(HCl)_2(H_2O)$ and $HCl(H_2O)_2$ are given in (a), (b) and (c). Also, the hydrogen bonded distances of the hydrogen atom of the centre HCl to the oxygen atom of the adjacent water molecule are shown in the figure.

Reference:

(1) Grimme, S. Semiempirical GGA-type density functional constructed with a long-range dispersion correction. *J. Comput. Chem.* **2006**, *27*, 1787-1799.

(2) Martyna, G. J.; Klein, M. L.; Tuckerman, M. Nosé–Hoover chains: The canonical ensemble via continuous dynamics. *J. Chem. Phys.* **1992**, *97*, 2635-2643.

(3) Martyna, G. J.; Tuckerman, M. E. A reciprocal space based method for treating long range interactions in ab initio and force-field-based calculations in clusters. *J. Chem. Phys.* **1999**, *110*, 2810-2821.

(4) Gutberlet, A.; Schwaab, G.; Birer, Ö.; Masia, M.; Kaczmarek, A.; Forbert, H.; Havenith, M.; Marx, D. Aggregation-Induced Dissociation of HCl(H2O)4 Below 1 K: The Smallest Droplet of Acid. *Science* **2009**, *324*, 1545-1548.

(5) Flynn, S. D.; Skvortsov, D.; Morrison, A. M.; Liang, T.; Choi, M. Y.; Douberly, G. E.; Vilesov, A. F. Infrared Spectra of HCl−H2O Clusters in Helium Nanodroplets. *J. Phys. Chem. Lett.* **2010**, *1*, 2233-2238.

(6) Forbert, H.; Masia, M.; Kaczmarek-Kedziera, A.; Nair, N. N.; Marx, D. Aggregation-Induced Chemical Reactions: Acid Dissociation in Growing Water Clusters. *J. Am. Chem. Soc.* **2011**, *133*, 4062-4072.

(7) Sugawara, S.; Yoshikawa, T.; Takayanagi, T.; Tachikawa, M. Theoretical study on mechanisms of structural rearrangement and ionic dissociation in the HCl(H2O)4 cluster with path-integral molecular dynamics simulations. *Chem. Phys. Lett.* **2011**, *501*, 238-244.

(8) Walewski, Ł.; Forbert, H.; Marx, D. Quantum Induced Bond Centering in Microsolvated HCl: Solvent Separated versus Contact Ion Pairs. *J. Phys. Chem. Lett.* **2011**, *2*, 3069-3074.

(9) Letzner, M.; Gruen, S.; Habig, D.; Hanke, K.; Endres, T.; Nieto, P.; Schwaab, G.; Walewski, Ł.; Wollenhaupt, M.; Forbert, H.; Marx, D.; Havenith, M. High resolution spectroscopy of HCl–water clusters: IR bands of undissociated and dissociated clusters revisited. *J. Chem. Phys.* **2013**, *139*, -.

(10) Walewski, Ł.; Forbert, H.; Marx, D. Revealing the Subtle Interplay of Thermal and Quantum Fluctuation Effects on Contact Ion Pairing in Microsolvated HCl. *ChemPhysChem* **2013**, *14*, 817-826.

(11) Mukamel, S. *Principles of Nonlinear Optical Spectroscopy*; Oxford: London, 1995.

(12) Kwac, K.; Lee, H.; Cho, M. Non-Gaussian statistics of amide I mode frequency fluctuation of N-methylacetamide in methanol solution: Linear and nonlinear vibrational spectra. *J. Chem. Phys.* **2004**, *120*, 1477-1490.

(13) Cho, M. Coherent Two-Dimensional Optical Spectroscopy. *Chem. Rev.* **2008**, *108*, 1331-1418.